

Published in final edited form as:

Exp Neurol. 2010 December ; 226(2): 265–273. doi:10.1016/j.expneurol.2010.08.024.

¹⁸F-FECNT: Validation as PET Dopamine Transporter Ligand in Parkinsonism

Gunasingh Masilamoni, PhD¹, John Votaw, PhD^{1,3}, Leonard Howell, PhD¹, Rosa M. Villalba, PhD¹, Mark Goodman, PhD^{1,3}, Ronald J Voll, PhD.³, Jeffrey Stehouwer, PhD.³, Thomas Wichmann, MD^{1,2}, and Yoland Smith, PhD^{1,2}

¹Yerkes National Primate Research Center, Emory University, Atlanta, GA, USA

²Department of Neurology, Emory University, Atlanta, GA, USA

³Department of Radiology, Emory University, Atlanta, GA, USA

Abstract

The positron emission tomography (PET) tracer 2β-carbomethoxy-3β-(4-chlorophenyl)-8-(2-[¹⁸F]-fluoroethyl)-nortropine (¹⁸F-FECNT) is a highly specific ligand for dopamine transporter (DAT) that yields higher peak striatum-to-cerebellum ratios and offers more favorable kinetics than most ¹⁸F-radiolabeled DAT ligands currently available. The goal of this study is to validate the use of ¹⁸F-FECNT as a PET radiotracer to assess the degree of striatal dopamine terminals denervation and midbrain dopaminergic cell loss in MPTP-treated parkinsonian monkeys. Three rhesus monkeys received weekly injections of MPTP (0.2-0.5 mg/kg) for 21 weeks, which resulted in the progressive development of a moderate level of parkinsonism. We carried out ¹⁸F-FECNT PET at baseline (twice; ten weeks apart) and at week 21 post-MPTP injections. Postmortem stereological cell counts of dopaminergic neurons in the ventral midbrain, and intensity measurements of DAT and tyrosine hydroxylase (TH) immunoreactivity in the striatum were performed and correlated with striatal and ventral midbrain PET data. Three additional monkeys were used as controls for midbrain dopaminergic cell counts, and striatal DAT or TH immunoreactivity measurements. The correlation and coefficient of variance between ¹⁸F-FECNT test-retest specific uptake ratios were 0.99 (R²) and 2.65%, respectively. The ¹⁸F-FECNT binding potential of the ventral midbrain and striatal regions was tightly correlated with postmortem stereological cell counts of nigral dopaminergic neurons (R² = 0.91), and striatal DAT (R² = 0.83) or TH (R² = 0.88) immunoreactivity intensity measurements. These findings demonstrate that ¹⁸F-FECNT is a highly sensitive PET imaging ligand to quantify both striatal dopamine denervation and midbrain dopaminergic cell loss associated with parkinsonism.

Keywords

Parkinson's disease; brain imaging; transporter; dopamine; striatum; MPTP; monkey; primate; substantia nigra; midbrain; animal model

© 2010 Elsevier Inc. All rights reserved.

Corresponding Author: Yoland Smith, PhD Yerkes National Primate Research Center Emory University 954 Gatewood Rd NE Atlanta, GA 30329 USA ysmit01@emory.edu Tel: (404) 727 7519.

Publisher's Disclaimer: This is a PDF file of an unedited manuscript that has been accepted for publication. As a service to our customers we are providing this early version of the manuscript. The manuscript will undergo copyediting, typesetting, and review of the resulting proof before it is published in its final citable form. Please note that during the production process errors may be discovered which could affect the content, and all legal disclaimers that apply to the journal pertain.

INTRODUCTION

Dysregulation of dopaminergic transmission in the basal ganglia has been implicated in brain disorders such as Parkinson's disease (PD), depression, addiction, schizophrenia, attention deficit hyperactivity disorder, and Tourette syndrome (Badgaiyan et al., 2009; Costa et al., 2009; Wichmann and DeLong, 2003). The homeostasis of dopaminergic transmission is controlled via the reuptake of extracellular dopamine (DA) by the plasma membrane-bound dopamine transporter (DAT) (Amara and Sonders, 1998; Kuhar et al., 1990). DAT is a member of a large family of Na⁺/Cl⁻-dependent transporters that also includes transporters for serotonin (SERT), norepinephrine (NET), GABA, and others (Amara and Sonders, 1998; Giros and Caron, 1993; Torres et al., 2003). Because DAT is expressed exclusively in DA neurons, it can be used as a specific marker of these neuronal cell bodies and their terminals in the CNS. The highest expression level of brain DAT is found in the striatum, followed by the olfactory tubercle, hypothalamus, and prefrontal cortex. Other areas, including the cerebellum are virtually devoid of DAT (Ciliax et al., 1995; Hoffman et al., 1998).

Several radiotracers have been developed to monitor and quantify DAT distribution in PD. Positron emission tomography (PET) is the most sensitive quantitative *in vivo* imaging approach that offers the highest level of spatial resolution (<2.0mm) to determine brain distribution of ligand-labeled endogenous neurochemical elements. Compared with other radionuclides, ¹⁸F-radiolabeled PET ligands are advantageous because their long half life (110 min) allows sufficient time for *ex vivo* synthesis of the tracer molecule, and reliable equilibration of *in vivo* uptake in the brain.

The PET tracer 2β-carbomethoxy-3β-(4-chlorophenyl)-8-(2-[¹⁸F]-fluoroethyl)-nortropine (¹⁸F-FECNT) is a useful tool for *in vivo* estimation of striatal DAT occupancy in monkey and human brains (Davis et al., 2003; Votaw et al., 2002) because it has a high binding affinity, strong selectivity and favorable kinetics towards DAT compared with other ¹⁸F-radiolabeled DAT ligands (Goodman et al., 2000; Honer et al., 2006). However, the use of this ligand as a clinical marker for the state of the DA system is highly dependent on the reproducibility and specificity of the scanning results for the DA system; two parameters that have not yet been adequately characterized.

The 1-methyl-4-phenyl-1,2,3,6-tetrahydropyridine (MPTP)-treated monkey is the best model to validate new PET ligands to monitor DAT changes during the development of parkinsonism (Ashkan et al., 2007; Pate et al., 1993; Poyot et al., 2001). Monkeys treated with MPTP display motor symptoms of parkinsonism, respond to dopaminergic treatments, and develop dyskinesias in response to L-DOPA therapy (Jenner, 2003). ¹⁸F-FDOPA has been the most frequently used ligand for noninvasive measurements of DA neuronal loss in PD, but DAT markers are more reliable ligands than ¹⁸F-FDOPA to assess the level of striatal dopamine-containing terminals, particularly in early PD state (see review in Dorsey et al., 2008, Pavese and Brooks 2009).

The objective of this study is to assess the test-retest reproducibility and pathological validity of ¹⁸F-FECNT as a PET radiotracer to localize and quantify DAT in the striatum and the ventral midbrain of parkinsonian monkeys chronically treated with a low dose MPTP regimen to mimic the slow and progressive degeneration that occurs in idiopathic PD.

MATERIALS AND METHODS

Experimental design

Six adult female rhesus macaque monkeys (*Macaca mulatta*, 4.5–8.5 kg) were used in this study. All experiments were approved by the Animal Care and Use Committee of Emory University. The six monkeys were divided into two groups. Group 1 consisted of 3 animals which first underwent base line PET scans and behavioral observations (see below), and then received weekly injections of MPTP (0.2-0.5 mg/kg i.m.; Sigma-Aldrich, St-Louis, MO) for 21 weeks (Fig.1). During the course of the MPTP injections, the monkeys progressively developed parkinsonian symptoms. At the end of the MPTP injection protocol another PET scan was performed, followed by termination of the experiment. Group 2 consisted of 3 untreated monkeys which served as controls for the postmortem dopaminergic cell counts and striatal densitometry measurement of DAT and TH immunoreactivity.

PET imaging

PET scans were performed at 3 different time points (Fig. 1). All PET data were collected with a Siemens Focus 220 micro-PET scanner at the Yerkes Center brain imaging facility.

The first two scans were achieved 10 weeks apart prior to the MPTP treatment to collect baseline data and to examine test-retest reproducibility of ^{18}F -FECNT PET scans. The third PET scan was performed at the end of MPTP injections. Data from this final scan were correlated with parkinsonian motor scores (see below), and levels of striatal immunoreactivity and nigral stereological cell counts obtained from TH- or DAT-immunostained material.

The monkeys were fasted for 12 h prior to the PET studies. The animals were initially anesthetized with an intramuscular injection of Telazol (3 mg/kg), and then maintained on a mixture of 1% isoflurane and 5% oxygen gas throughout the imaging session. Respiratory parameters, blood pressure, pulse rate and rectal temperature were monitored during the procedure. A 15 min transmission scan was obtained for attenuation correction, then a slow bolus of approximately 5.0 mCi of ^{18}F -FECNT (specific activity 1.5 Ci/ μmol) was injected over 5-6 min at a rate of 1.0 ml/min. The scanning began at the same time as the radiotracer injection. The initial acquisition was a 28-frame dynamic sequence, starting with 30-s scans and ending with 20 min scans (total duration, 110 min). All images were reconstructed using the manufacturer supplied software with measured attenuation correction, zoom factor 8, and Shepp-Logan reconstruction filter cut-off at 1 cycle/cm. The axial slice thickness was 3.375 mm. All images were decay-corrected to the time of injection. For the generation of time-activity curves for each monkey, the three different PET images (test, re-test and final PET scans) were superimposed using IDL software (ITT Visual Information Solutions, Boulder, CO), and averaged. Regions of interest (ROIs) were manually drawn on the average image of each hemisphere, delimiting the following striatal regions: putamen/associative (PA), putamen/motor (PM), putamen/limbic (PL), caudate nucleus/associative (CA) nucleus accumbens/limbic (AL), as well as the substantia nigra (SN) (Fig. 2a-d). The manually drawn ROIs on the average image were then superimposed onto the individual images, to obtain time-activity curves.

An estimate of specific binding for each region was calculated by subtracting the DAT-free cerebellum value from that measured in striatal and nigral ROIs after the system reached quasi-equilibrium, then divided by the cerebellum measurement (see Votaw et al., 2002 for more details). The value obtained through these calculations is termed specific uptake ratio (SUR) throughout the manuscript. The absolute difference of the quantitative parameters between the test and retest values divided by their average were taken as a reproducibility

index of the measurements (Okauchi et al., 2001). One-way ANOVA was used to determine significance of differences between average SUR.

Behavioral observations

Changes in the animal's behavioral state were documented using observation in a behavioral observation cage. One of the side walls of the cage is made of Plexiglas for easy visibility of the monkey. The cage is equipped with eight infrared beams for automated activity monitoring by counting beam breaks with an attached computer. Four of these beams are arranged in a square design between the back and front of the cage, and four additional beams, arranged in a similar manner, between the two sides of the cage. The animal's spontaneous behavior was assessed with this device for 15-min periods. In addition, ongoing monkey movements were videotaped and monitored by an observer, who pressed buttons on a keypad each time the monkey moved its extremities. Counts of the number of button presses quantify the amount of movement.

Animal perfusion

At the end of the experiments, monkeys were anesthetized with an overdose of pentobarbital (100 mg/kg, i.v.), and perfused transcardially with a mixture of paraformaldehyde and glutaraldehyde. After perfusion, the brains were cut into 10 mm-thick blocks that were further sectioned into 50- μ m slices for immunostaining and cell counting procedures.

Immunostaining

Striatal and midbrain sections of untreated and MPTP-treated monkeys were immunostained with specific monoclonal rat anti-DAT or mouse anti-TH antibodies (Millipore, Temecula, CA, USA; Catalog number MAB 369 and 318, respectively) at a concentration of 1:1000. We used highly specific mouse monoclonal calbindin D28K (CB) antibodies at a concentration of 1:4000 (Sigma, Catalog number C9848) to delineate the borders between the ventral and dorsal tiers of the substantia nigra pars compacta (SNc-v versus SNc-d). The immunoperoxidase ABC method was used to localize the different markers according to procedures described in previous studies (Smith and Bolam 1991). DAT and TH immunoreactivity in the striatum was quantified using the MCID program (Imaging Research Inc., St. Catharines, Ontario, Canada). Macroscopic images were acquired with a Cool SNAPcf photometrics camera. The ROIs were outlined (see Fig.2a-d) on a computer screen, and the average pixel density measured and expressed as relative optical density (ROD). Mean values were calculated, using one out of every 12 sections. With this measuring scheme, 5-7 sections were used per ROI in each brain hemisphere.

Stereological estimation of TH-positive neurons

The unbiased stereological estimation of the total number of TH-positive cells in SNc-v, SNc-d, and VTA was analyzed using the optical fractionator principle (StereoInvestigator, MicroBrightField, Inc., Williston, VT). The random systematic sampling of counting areas was done using the Leica DMR microscope. First, we took low power micrographs (1.25X) of TH- and CB-immunostained ventral midbrain sections, and manually delineated the borders of SNc-v, SNc-d, and VTA, based on the presence and absence of CB-positive neurons. Then, the borders of the different ventral midbrain regions were manually delineated on TH-immunolabeled slides adjacent to those immunostained for CB.

Counts of TH-positive cells were generated using a 100X oil-immersion objective. To perform unbiased stereology, counting frames (65 \times 65 μ m) were randomly placed by the stereology software within the chosen ROI. The software also controlled the position of the x-y stage of the microscope, so that the entire brain region could be scanned by successively

meandering between counting frames. On average, 12 sections were analyzed and approximately 300 cells were counted in controls. The software calculated the estimated total number of cells in the SNc-v, SNc-d, and VTA per hemisphere.

RESULTS

¹⁸F-FECNT Time-activity Curves in ROIs

Representative baseline ¹⁸F-FECNT time-activity curves for the different ROIs examined (PA, PM, PL, CA, AL, SN and cerebellum) are shown in Figure 3a. After intravenous administration of ¹⁸F-FECNT, there was a rapid accumulation of radioactivity in all ROIs, but at varying degrees according to the densities of DAT. The radioactivity in the cerebellum dropped sharply 10 min after the bolus injection of ¹⁸F-FECNT and remained low at all time points thereafter. Although lower than striatal ROIs, the ventral midbrain reached maximal uptake between 30 and 45 min after injection, at a level that was significantly higher than the cerebellum. These findings also demonstrate that the quasi-equilibrium of uptake was reached in brain regions with low DAT density, like the cerebellum and SN, earlier than in DAT-enriched striatal areas in which uptake quasi-equilibrium was reached 90-110 min post-injection (Fig. 3a). The highest level of radioactivity was measured in the PA, followed by CA, PM, AL, PL and SN. To determine statistical differences between the uptake values collected in each ROI, the average measurements of the three last time points (95, 105, 115 min.) were calculated and statistically compared using ANOVAs, and Tukey's Post-hoc tests. The uptake measurements in limbic areas (AL, PL) were significantly lower than those in other striatal regions (PA, CA, PM), ($p < 0.05$), but significantly higher than those in the SNc ($p < 0.001$) (Fig. 3d). The striatal and nigral uptake values were significantly higher than those in the cerebellum ($p < 0.0001$).

Test-retest reproducibility of ¹⁸F-FECNT PET scan specific uptake ratio measurements

A high level of reproducibility of SUR measurements across experiments in the same animal is a prerequisite to the use of this ligand in longitudinal studies. We assessed the reproducibility of the SUR of ¹⁸F-FECNT PET measurements gathered from the different ROIs in normal monkeys (Figures 2a-d, 3b). The SUR peak values in the different striatal ROIs and the SNc displayed a gradual increase up to about 80-90 min post-injection and then stabilized (Supplementary Fig.1). Thus, to compare test-retest values for SUR of ¹⁸F-FECNT PET measurements that were collected 10 weeks apart, the peak measurements collected at 95, 105 and 115 min post-injections were averaged and used for statistical analysis (Fig. 3b). This analysis did not reveal any significant difference in the test-retest SUR values across experimental sessions (10 weeks apart from each other) within the same hemisphere in individual monkeys (Fig. 3b). The ¹⁸F-FECNT test and retest PET scan SUR values were tightly correlated ($r=0.99$, Fig. 3c). These results demonstrate that ¹⁸F-FECNT has high reproducibility and negligible variability for longitudinal PET imaging measurements of DAT binding in the normal monkey brain.

Relationship between changes in ¹⁸F-FECNT striatal specific uptake ratio and behavioral impairments in MPTP-treated parkinsonian monkeys

In humans, the severity of motor symptoms of PD, namely resting tremor, rigidity, and bradykinesia is correlated with the degree of dopamine denervation in the motor territory of the putamen (Bernheimer et al, 1973). To examine the relationship between measurements of striatal ¹⁸F-FECNT PET binding and the severity of motor symptoms in parkinsonism, we correlated ¹⁸F-FECNT PET imaging measurements in the PM ROI of parkinsonian monkeys with the results of quantitative measurements of motor activity as described in the method section. The different measures of behavior (infrared beam breaks, and activity

counts based on direct observations) are closely correlated (Supplementary Fig. 2). After 21 MPTP injections, the monkeys showed different degrees of motor impairment severity (70-90% reduction in total movements) that were matched with corresponding decrease in SUR values of ^{18}F -FECNT PET in PM (Fig. 4).

Relationship between ^{18}F -FECNT specific uptake ratio and postmortem DAT and TH immunoreactivity

We correlated the post-MPTP ^{18}F -FECNT SUR values with the intensity measurements of DAT and TH immunoreactivity in striatal tissue. Fig. 5a-l shows examples of *in vivo* ^{18}F -FECNT PET images and *ex vivo* DAT- and TH-ir, collected in corresponding striatal regions of control and MPTP-treated monkeys. These results demonstrate that MPTP treatment induced a variable degree of DA denervation of all striatal regions, in both hemispheres (Fig. 5a-l). The post-commissural putamen (ROI: PM) was the most severely depleted region followed by associative and limbic territories (PA, CA, PL and AL). Based on this heterogeneous pattern of striatal dopamine denervation, we performed a correlation analysis between the FECNT-SUR from *in vivo* PET images with their corresponding *ex vivo* densitometry measurements for a series of striatal ROIs of which the limits could be clearly delineated from PET images. The results of this analysis show that the degree of changes in ^{18}F -FECNT SUR was tightly correlated with the densitometry measurements of DAT and TH ir in all striatal territories examined (Fig. 5m,n and supplementary Fig. 3a,b).

^{18}F -FECNT specific uptake ratio and Midbrain Dopaminergic Cell Loss in MPTP-treated Monkeys

The ^{18}F -FECNT PET imaging measurements and the intensity levels of postmortem DAT and TH immunostaining demonstrated a significant loss of uptake and immunoreactivity in the ventral midbrain of parkinsonian monkeys, compared with baseline values from untreated animals (Fig. 6a-d). The decrease in the number of TH-immunoreactive neurons was more pronounced in the SNC-v ($68 \pm 17\%$ loss) than in the SNC-d ($57 \pm 21\%$) and VTA ($52 \pm 14\%$). On the other hand, the ^{18}F -FECNT SUR in the ventral midbrain was decreased by $66 \pm 14\%$ (Fig. 6a,c). The correlation coefficient analysis showed that SNC ^{18}F -FECNT SUR is tightly correlated with the stereological cell count measurements of TH-positive neurons in the SNC-v (Fig. 6e). In addition, the extent of ventral midbrain neuronal degeneration was predicted from their corresponding striatal ^{18}F -FECNT SUR reduction. For example, the percentage of neuronal loss in the VTA was tightly correlated with ^{18}F -FECNT SUR of AL territory ($R^2=0.85$; Fig. 6f).

DISCUSSION

The findings of this study demonstrate that PET imaging of the DAT ligand ^{18}F -FECNT is a highly sensitive approach that provides highly reproducible assessments of the integrity of the nigrostriatal dopaminergic system at both striatal and midbrain levels in MPTP-treated monkeys.

Overall, the distribution of ^{18}F -FECNT binding in the monkey brain reported in this study is consistent with previous data in monkeys and humans (Davis et al., 2003; Votaw et al., 2002). FECNT is highly selective for DAT, as demonstrated in previous *in-vitro* competitive binding experiments in transfected murine kidney cells which compared FECNT with the labeled serotonin and norepinephrine transporter ligands [^3H]citalopram and [^3H]nisoxetine. ^{18}F -FECNT was found to have 25 and 156 fold greater affinity for human (h) hDAT than for hSERT and hNET, respectively (Goodman et al., 2000). The striatum/cerebellum ratios of ^{18}F -FECNT uptake (≈ 12) reported here are much higher than those of other DAT selective compounds (^{18}F -FCT, ^{18}F -S-FIPCT, ^{18}F -FPCIT, ^{18}F -FPCT, ^{18}F -(R)-

FIPCT and ^{18}F -CFT) that have been used in primates (Mach et al., 2000; Kazumata et al., 1998; Goodman et al., 1997; Stout et al., 1999; Xing et al., 2000). The significantly lower ^{18}F -FECNT SUR values in limbic ROIs are consistent with the fact that these areas receive their dopaminergic innervation from the VTA, which expresses less DAT than dopaminergic fibers originating in the SNc-v (Shimada et al., 1992). However, this difference was not detected in the postmortem immunoreactivity densitometry analysis (Supplementary Fig.4 and Ciliax et al., 1995). Together, these data provide strong evidence that ^{18}F -FECNT is an excellent candidate for *in-vivo* PET imaging of DAT in primates.

In this study, SUR was used as an index of FECNT binding because it can be objectively calculated for each ROI. In the limiting case of reaching steady state, this ratio is equivalent to the binding potential (Votaw et al., 2002), thereby providing a measure highly correlated with DAT density that can easily be calculated with little variability. Our data show that in all regions, except SNC, the ^{18}F -FECNT uptake values are very close to steady-state by the end of the data collection (115 minutes post-injection). Although the reason for the continued decrease in SNC uptake remains unclear, it may be related to low DAT density in the midbrain regions compared with the striatum (Ciliax et al., 1995). Despite this limited stability, it is noteworthy that the test-retest variability in FECNT uptake for all regions, including the SNC, is very low. Furthermore, these findings are consistent with those of a recent human study using ^{11}C -PE2I radiotracer as DAT ligand (Hirvonen et al., 2008). However, because of its longer half-life, the ^{18}F offers significant advantages over the short 20 min half-life of carbon-11. Together these observations provide additional evidence for the use of ^{18}F -FECNT as a highly reliable ligand to assess changes in DAT at both striatal and ventral midbrain levels in parkinsonism or other pathologic conditions.

The negligible differences of SUR values in the test–retest PET scans ($\approx 2\%$) demonstrate the high level of reproducibility of ^{18}F -FECNT binding in the striatum and midbrain. This test–retest reproducibility of ^{18}F -FECNT PET scan in striatal and extrastriatal regions is far superior to that reported for other DAT imaging radiotracers, such as ^{11}C -PE2I ($\approx 10\%$), ^{11}C -L-DOPA ($\approx 5\%$) (Nagai et al., 2007) and ^{18}F -CFT ($\approx 8\%$) (Goodman et al., 1997). These findings suggest that ^{18}F -FECNT and SUR might be a more reliable candidate and analysis method than other ligands for use in *in vivo* DAT mapping in the context of longitudinal clinical studies of drug effects or disease progression in parkinsonian and other patients.

The (negative) correlation between the level of ^{18}F -FECNT SUR in the sensorimotor putamen and the severity of parkinsonian behavior is consistent with that demonstrated in human studies (Davis et al., 2003), thereby providing evidence that ^{18}F -FECNT is a reliable PET radiotracer to assess the severity of the degeneration of the nigrostriatal system and the resulting motor symptomatology in PD.

^{18}F -DOPA PET was the first neuroimaging technique validated for the assessment of presynaptic dopaminergic integrity. However, the validation of *in vivo* ^{18}F -FDOPA PET measurements in the striatum as an index of DA cell counts in the SNc has been controversial (Pate et al., 1993; Snow et al., 1993; Yee et al., 2001). In addition, because the uptake of ^{18}F -DOPA is affected by changes in dopamine metabolism, it may underestimate the degenerative process due to compensatory up-regulation of aromatic acid decarboxylase (AADC) in remaining dopaminergic terminals, particularly in early stages of disease (Ribeiro et al., 2002). In contrast, ^{18}F -FECNT DAT uptake reflects binding to dopamine transporters that are less affected by metabolic factors, thus providing a more reliable index of the (anatomic) abundance of striatal dopamine terminals, especially at early stages of the disease (Ito et al., 1999).

In the present study, the DA neuronal loss in the VTA was predicted from the ^{18}F -FECNT SUR reduction of its corresponding striatal region, the nucleus accumbens (ROI=AL). However, other authors did not find correlation between *in vivo* single photon emission computed tomography (SPECT) measures of striatal DAT and nigral stereological cell counts in mice and monkey models of PD (Alvarez-Fischer et al., (2007; Scheller et al., 2007). Two main explanations could be suggested for these discrepancies. First, the chronic nature of the MPTP exposure used to intoxicate monkeys in our study versus a much more acute striatal dopamine denervation induced in these previous studies. Second, the PET imaging method offers a much higher spatial resolution than SPECT to assess regional changes in DAT ligand binding. Thus, although tentative correlations between levels of striatal DAT binding and the relative degree of midbrain neuronal loss can be made, it is imperative that such extrapolation relies on the use of highly sensitive ligands visualized with an imaging method that offers the highest possible spatial resolution. Because striatal dopaminergic denervation precedes nigral neuronal loss (Bernheimer et al., 1991; Lee et al., 2000), striatal DAT radiotracer uptake is not a sensitive biomarker to predict the extent of nigral neuronal loss at early stages of the disease (Poyot et al., 2001). The correlation between *midbrain* ^{18}F -FECNT SUR and the number of DA neurons in the SNc in MPTP-treated monkeys shown in our study is therefore highly relevant, and offers the possibility to directly monitor both striatal and nigral dopaminergic denervation during disease progression, a valuable asset for neuroprotective studies in parkinsonian patients.

Therefore, based on its high specificity for DAT over other monoamine transporters, high degree of test-retest reproducibility and excellent sensitivity, ^{18}F -FECNT should be considered as the best PET imaging tracers available to visualize and quantify changes in DA cell counts, and striatal dopamine innervation in PD.

Supplementary Material

Refer to Web version on PubMed Central for supplementary material.

Acknowledgments

This work was supported by a grant from the National Parkinson Foundation and the Yerkes Primate Center NIH/NCRR base grant (RR00165). Thanks are due to Susan Jenkins for technical assistance and Jim Bogenpohl, Xing Hu and Adriana Galvan for training with monkey behavior. The authors are also grateful to Professor Carlos Avendano from the University Autonoma in Madrid who has helped with the design and interpretation of stereological data.

REFERENCES

- Alvarez-Fischer D, Blessmann G, Trosowski C, Béhé M, Schurrat T, Hartmann A, Behr TM, Oertel WH, Höglinger GU, Höffken H. Quantitative [(123)I]FP-CIT pinhole SPECT imaging predicts striatal dopamine levels, but not number of nigral neurons in different mouse models of Parkinson's disease. *Neuroimage*. 2007; 38:5–12. [PubMed: 17716921]
- Amara SG, Sonders MS. Neurotransmitter transporters as molecular targets for addictive drugs. *Drug Alcohol Depend*. 1998; 51:87–96. [PubMed: 9716932]
- Ashkan K, Wallace BA, Mitrofanis J, Pollo C, Brard PY, Fagret D, Benabid AL. SPECT imaging, immunohistochemical and behavioural correlations in the primate models of Parkinson's disease. *Parkinsonism Relat Disord*. 2007; 13:266–75. [PubMed: 17196871]
- Badgaiyan RD, Fischman AJ, Alpert NM. Dopamine release during human emotional processing. *Neuroimage*. 2009; 47:2041–45. [PubMed: 19524047]
- Bernheimer H, Birkmayer W, Hornykiewicz O, Jellinger K, Seitelberger F. Brain dopamine and the syndromes of Parkinson and Huntington. Clinical, morphological and neurochemical correlations. *J Neurol Sci*. 1973; 20:415–55. [PubMed: 4272516]

- Ciliax BJ, Heilman C, Demchyshyn LL, Pristupa ZB, Ince E, Hersch SM, Niznik HB, Levey AI. The dopamine transporter: immunochemical characterization and localization in brain. *J Neurosci.* 1995; 15:1714–1723. [PubMed: 7534339]
- Costa A, Peppe A, Dell’Agnello G, Caltagirone C, Carlesimo GA. Dopamine and cognitive functioning in de novo subjects with Parkinson’s disease: effects of pramipexole and pergolide on working memory. *Neuropsychologia.* 2009; 47:1374–81. [PubMed: 19428401]
- Davis MR, Votaw JR, Bremner JD, Byas-Smith MG, Faber TL, Voll RJ, Hoffman JM, Grafton ST, Kilts CD, Goodman MM. Initial human PET imaging studies with the dopamine transporter ligand 18F-FECNT. *J Nucl Med.* 2003; 44:855–61. [PubMed: 12791810]
- Dorsey, ER.; Holloway, RG.; Ravina, BM.; Factor, SA. Status of biological markers. In: Weiner, WJ., editor. *Parkinson’s Disease-Diagnosis and Clinical Management.* Demos; New York: 2008. p. 277-284.
- Giros B, Caron MG. Molecular characterization of the dopamine transporter. *Trends Pharmacol Sci.* 1993; 14:43–49. [PubMed: 8480373]
- Goodman MM, Keil R, Shoup TM, Eshima D, Eshima L, Kilts C, Votaw J, Camp VM, Votaw D, Smith E, Kung MP, Malveaux E, Watts R, Huerkamp M, Wu D, Garcia E, Hoffman JM. Fluorine-18-FPCT: a PET radiotracer for imaging dopamine transporters. *J Nucl Med.* 1997; 38:119–26. [PubMed: 8998165]
- Goodman MM, Kilts CD, Keil R, Shi B, Martarello L, Xing D, Votaw J, Ely TD, Lambert P, Owens MJ, Camp VM, Malveaux E, Hoffman JM. 18F-labeled FECNT: a selective radioligand for PET imaging of brain dopamine transporters. *Nucl Med Biol.* 2000; 27:1–12. [PubMed: 10755640]
- Herkenham M, Little MD, Bankiewicz K, Yang SC, Markey SP, Johannessen JN. Selective retention of MPP+ within the monoaminergic systems of the primate brain following MPTP administration: an in vivo autoradiographic study. *Neuroscience.* 1991; 40:133–58. [PubMed: 2052148]
- Hirvonen J, Johansson J, Teräs M, Oikonen V, Lumme V, Virsu P, Roivainen A, Någren K, Halldin C, Farde L, Hietala J. Measurement of striatal and extrastriatal dopamine transporter binding with high-resolution PET and [11C]PE2I: quantitative modeling and test-retest reproducibility. *J Cereb Blood Flow Metab.* 2008; 28:1059–69. [PubMed: 18183028]
- Hoffman BJ, Hansson SR, Mezey E, Palkovits M. Localization and dynamic regulation of biogenic amine transporters in the mammalian central nervous system. *Front Neuroendocrinol.* 1998; 19:187–231. [PubMed: 9665836]
- Honer M, Hengerer B, Blagoev M, Hintermann S, Waldmeier P, Schubiger PA, Ametamey SM. Comparison of [18F]FDOPA, [18F]FMT and [18F]FECNT for imaging dopaminergic neurotransmission in mice. *Nucl Med Biol.* 2006; 33:607–14. [PubMed: 16843835]
- Ito Y, Fujita M, Shimada S, Watanabe Y, Okada T, Kusuoka H, Tohyama M, Nishimura T. Comparison between the decrease of dopamine transporter and that of L-DOPA uptake for detection of early to advanced stage of Parkinson’s disease in animal models. *Synapse.* 1999; 31:178–85. [PubMed: 10029235]
- Jenner P. The MPTP-treated primate as a model of motor complications in PD: primate model of motor complications. *Neurology.* 2003; 23, 61:S4–11. [PubMed: 14504374]
- Kazumata K, Dhawan V, Chaly T, Antonini A, Margouleff C, Belakhlef A, Neumeier J, Eidelberg D. Dopamine transporter imaging with fluorine-18-FPCIT and PET. *J Nucl Med.* 1998; 39:1521–30. [PubMed: 9744335]
- Kordower JH, Herzog CD, Dass B, Bakay RA, Stansell J 3rd, Gasmi M, Bartus RT. Delivery of neurturin by AAV2 (CERE-120)-mediated gene transfer provides structural and functional neuroprotection and neurorestoration in MPTP-treated monkeys. *Ann Neurol.* 2006; 60:706–15. [PubMed: 17192932]
- Kuhar MJ, Sanchez-Roa PM, Wong DF, Dannals RF, Grigoriadis DE, Lew R, Milberger M. Dopamine transporter: biochemistry, pharmacology and imaging. *Eur Neurol.* 1990; 30:15–20. [PubMed: 2178937]
- Lee CS, Samii A, Sossi V, Ruth TJ, Schulzer M, Holden JE, Wudel J, Pal PK, dela Fuente-Fernandez R, Calne DB, Stoessl AJ. In vivo positron emission tomographic evidence for compensatory changes in presynaptic dopamine nerve terminals in Parkinson’s disease. *Ann. Neurol.* 2000; 47:493–503.

- Mach RH, Nader MA, Ehrenkauser RL, Gage HD, Childers SR, Hodges LM, Hodges MM, Davies HM. Fluorine-18-labeled tropane analogs for PET imaging studies of the dopamine transporter. *Synapse*. 2000; 37:109–17. [PubMed: 10881032]
- Nagai Y, Obayashi S, Ando K, Inaji M, Maeda J, Okauchi T, Ito H, Suhara T. Progressive changes of pre- and post-synaptic dopaminergic biomarkers in conscious MPTP-treated cynomolgus monkeys measured by positron emission tomography. *Synapse*. 2007; 61:809–19. [PubMed: 17598150]
- Okauchi T, Suhara T, Maeda J, Kawabe K, Obayashi S, Suzuki K. Effect of endogenous dopamine on endogenous dopamine on extrastriated [¹¹C]FLB 457 binding measured by PET. *Synapse*. 2001; 41:87–95. [PubMed: 11400175]
- Parent A, Hazrati LN. Functional anatomy of the basal ganglia. I. The cortico-basal ganglia-thalamo-cortical loop. *Brain Res Brain Res Rev*. 1995; 20:91–127. [PubMed: 7711769]
- Pate BD, Kawamata T, Yamada T, McGeer EG, Hewitt KA, Snow BJ, Ruth TJ, Calne DB. Correlation of striatal fluorodopa uptake in the MPTP monkey with dopaminergic indices. *Ann Neurol*. 1993; 34:331–8. [PubMed: 8363350]
- Pavese N, Brooks DJ. Imaging neurodegeneration in Parkinson's disease. *Biochim Biophys Acta*. 2009; 1792:722–29. [PubMed: 18992326]
- Poyot T, Condé F, Grégoire MC, Frouin V, Coulon C, Fuseau C, Hinnen F, Dollé F, Hantraye P, Bottlaender M. Anatomic and biochemical correlates of the dopamine transporter ligand 11C-PE2I in normal and parkinsonian primates: comparison with 6-[¹⁸F]fluoro-L-dopa. *J Cereb Blood Flow Metab*. 2001; 21:782–92. [PubMed: 11435790]
- Ribeiro MJ, Vidailhet M, Loch C, Dupel C, Nguyen JP, Ponchant M, Dolle F, Peschanski M, Hantraye P, Cesaro P, Samson Y, Remy P. Dopaminergic function and dopamine transporter binding assessed with positron emission tomography in Parkinson disease. *Arch Neurol*. 2002; 59:580–586. [PubMed: 11939892]
- Scheller D, Chan P, Li Q, Wu T, Zhang R, Guan L, Ravenscroft P, Guigoni C, Crossman AR, Hill M, Bezard E. Rotigotine treatment partially protects from MPTP toxicity in a progressive macaque model of Parkinson's disease. *Exp Neurol*. 2007; 203:415–22. [PubMed: 17045989]
- Shimada S, Kitayama S, Walther D, Uhl G. Dopamine transporter mRNA: dense expression in ventral midbrain neurons. *Brain Res Mol Brain Res*. 1992; 13:359–62. [PubMed: 1352613]
- Smith Y, Bolam JP. Convergence of synaptic inputs from the striatum and the globus pallidus onto identified nigrocollicular cells in the rat: a double anterograde labelling study. *Neuroscience*. 1991; 44:45–73. [PubMed: 1722893]
- Snow BJ, Tooyama I, McGeer EG, Yamada T, Calne DB, Takahashi H, Kimura H. Human positron emission tomographic [¹⁸F]fluorodopa studies correlate with dopamine cell counts and levels. *Ann Neurol*. 1993; 34:324–30. [PubMed: 8363349]
- Stout D, Petric A, Satyamurthy N, Nguyen Q, Huang SC, Namavari M, Barrio JR. 2Beta-carbomethoxy-3beta-(4- and 2-[¹⁸F]fluoromethylphenyl) tropanes: specific probes for in vivo quantification of central dopamine transporter sites. *Nucl Med Biol*. 1999; 26:897–903. [PubMed: 10708303]
- Torres GE, Gainetdinov RR, Caron MG. Plasma membrane monoamine transporters: structure, regulation and function. *Nat Rev Neurosci*. 2003; 4:13–25. [PubMed: 12511858]
- Votaw JR, Howell LL, Martarello L, Hoffman JM, Kilts CD, Lindsey KP, Goodman MM. Measurement of dopamine transporter occupancy for multiple injections of cocaine using a single injection of [¹⁸F]FECNT. *Synapse*. 2002; 44:203–10. [PubMed: 11984856]
- Wichmann T, DeLong MR. Pathophysiology of Parkinson's disease: the MPTP primate model of the human disorder. *Ann N Y Acad Sci*. 2003; 991:199–213. [PubMed: 12846988]
- Yee RE, Irwin I, Milonas C, Stout DB, Huang SC, Shoghi-Jadid K, Satyamurthy N, Delanney LE, Togasaki DM, Farahani KF, Delfani K, Janson AM, Phelps ME, Langston JW, Barrio JR. Novel observations with FDOPA-PET imaging after early nigrostriatal damage. *Mov Disord*. 2001; 16:838–48. [PubMed: 11746613]
- Xing D, Chen P, Keil R, Kilts CD, Shi B, Camp VM, Malveaux G, Ely T, Owens MJ, Votaw J, Davis M, Hoffman JM, BaKay RA, Subramanian T, Watts RL, Goodman MM. Synthesis, biodistribution, and primate imaging of fluorine-18 labeled 2beta-carbo-1'-fluoro-2-

propoxy-3beta-(4-chlorophenyl)tr opanes. Ligands for the imaging of dopamine transporters by positron emission tomography. *J Med Chem.* 2000; 43:639–48. [PubMed: 10691690]

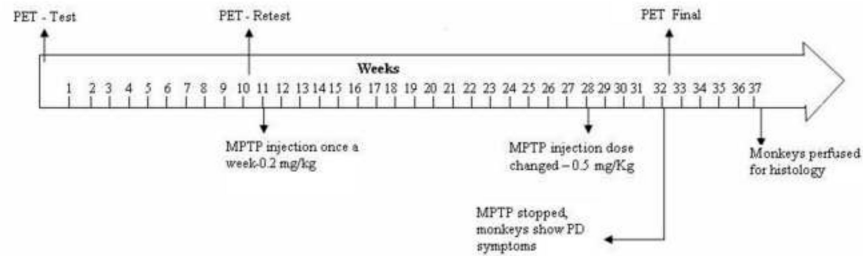


Fig. 1. Study design. After a few weeks of habituation to handling, transport and transfer in and out of the behavioral cages, monkeys (n=3) were subjected to a first ^{18}F -FECNT PET scan (PET I-Test). After ten weeks of basal behavioral monitoring, the monkeys were subjected to a second PET scan for retest to validate the reproducibility of baseline measurements of ^{18}F -FECNT binding (PET II-retest). A low dose regimen (0.2mg/kg, body wt., once a week) of MPTP administration started a week after the second PET scan for a period of 17 weeks. Between weeks 28 and 32, the dose of MPTP was increased to 0.5mg/kg body wt./week. The MPTP injections were stopped at week 32 when monkeys displayed moderate-severe parkinsonian symptoms. All monkeys were then subjected to a final PET scan. After 5 weeks of behavioral observation to ensure stability of the parkinsonian symptoms, the animals were perfusion-fixed for histological analysis.

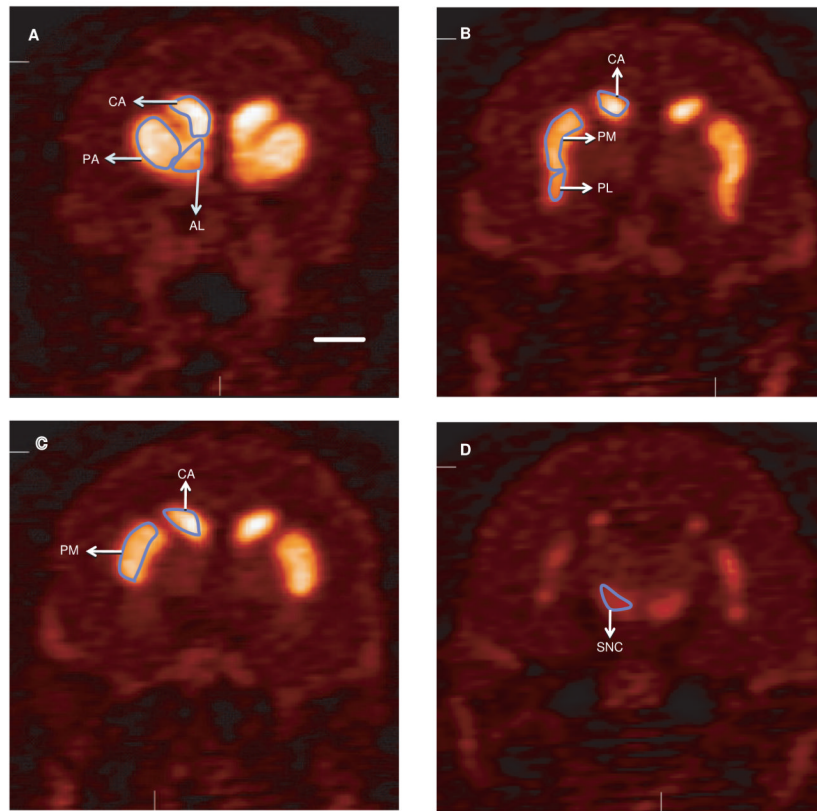
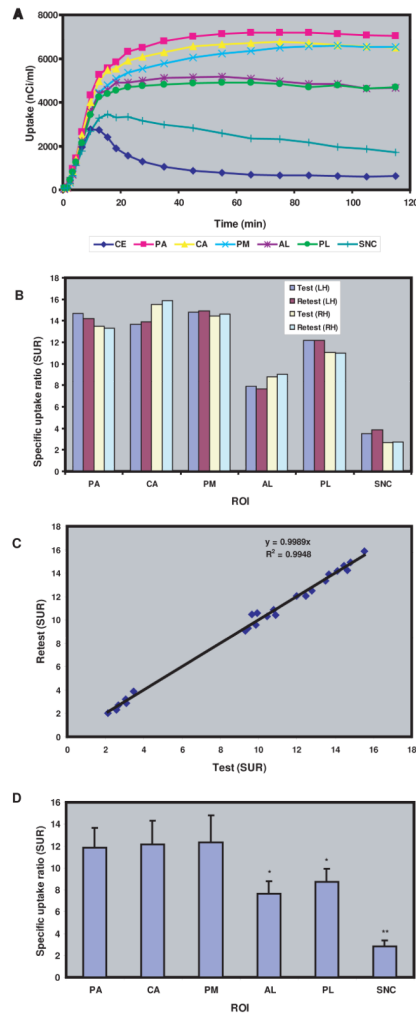


Fig. 2. ^{18}F -FECNT PET images of the different striatal functional territories of a control monkey. The delineation of these functional territories is based on the topography of corticostriatal projections in nonhuman primates (Parent and Hazrati, 1995). These functional areas were used as regions of interests (ROIs), for measurements of staining intensity in both ^{18}F -FECNT PET images and postmortem DAT- and TH-immunostained striatal sections of control and parkinsonian monkeys. Scale bar: 10 mm (valid for B-D).

**Fig.3.**

(A) Representative base line ^{18}F -FECNT time activity curves (TAC) for the different regions of interests (ROIs) examined in this study, i.e putamen associative (PA), putamen motor (PM), putamen limbic (PL), caudate nucleus (CA) accumbens limbic (AL) substantia nigra (SNC), and cerebellum (transporter free reference region) in rhesus monkey for a period of 120 minutes after administration of 5.6 mci of ^{18}F -FECNT. TAC reached their maximum values at 10, 45 and 90 min in the cerebellum, SNC and other ROIs, respectively. The highest level of radioactivity was measured in the PA, followed by PM, CA, PL, AL and SNC. (B) Representative test retest ^{18}F -FECNT specific uptake ration (SUR) of different ROIs in both hemispheres (LH: left hemisphere; RH: right hemisphere). A high level of reproducibility and negligible variability was found within inter-individual test–retest of ^{18}F -FECNT PET images. (C) Correlation between test retest ^{18}F -FECNT SUR of different ROIs in the left and right hemispheres of the 3 parkinsonian monkeys. Tight correlation coefficient was found between the ^{18}F -FECNT test and retest PET scans SUR values. (D) Average SUR showing that the limbic striatal areas (AL, PL) and the SNC displayed a significantly lower level of ^{18}F -FECNT binding than the motor (PM) and associative (PA, CA) striatal regions.

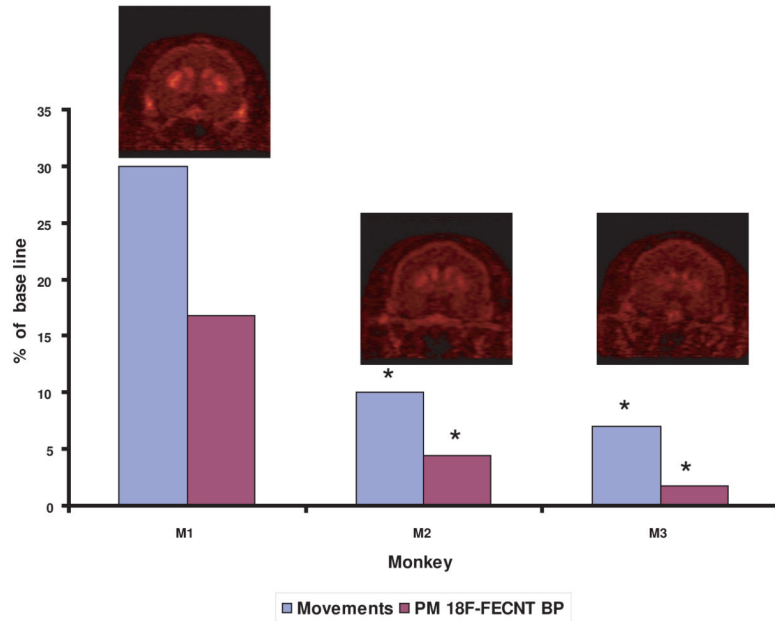


Fig. 4. Correlation between the respective level of ^{18}F -FECNT SUR in the sensorimotor putamen (ie ROI-PM) and the severity of parkinsonian motor impairments in MPTP-treated monkeys. Changes in both measures are displayed as percent changes from baseline values prior to the MPTP treatment. The decreased values in ^{18}F -FECNT radiotracer uptake in PM corresponds with the severity of motor impairments in these animals (M1, M2, M3 – 3 different monkeys). Asterisks indicate significant difference from values in monkey M1 ($P < 0.05$).

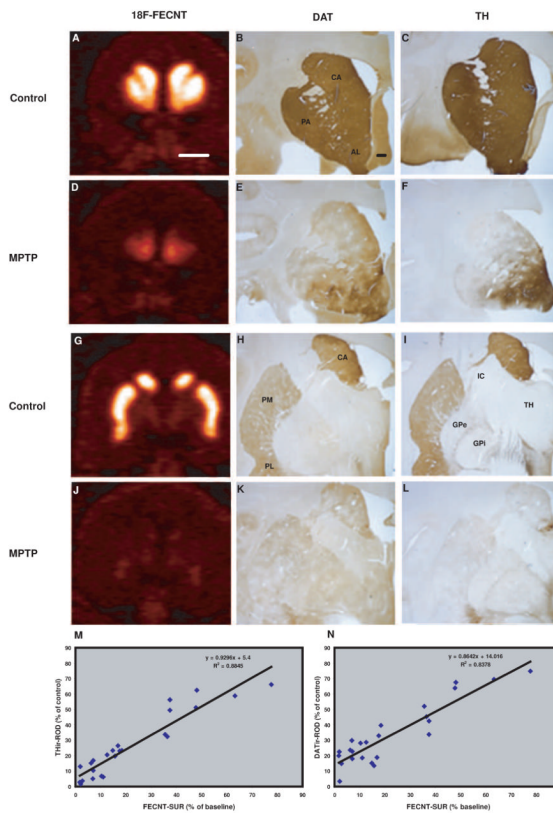


Fig. 5. Pre-commissural (A-F) and post-commissural (G-L) coronal planes of in-vivo ^{18}F -FECNT PET images compared with levels of dopamine transporter (DAT) (B,E,H,K) and tyrosine hydroxylase (TH) (C,F,I,L) immunoreactivity in control and parkinsonian monkeys. An almost complete and uniform depletion of ^{18}F -FECNT, DAT-ir and TH-ir was observed in the post commissural striatal regions, but less dopamine denervation was found in the accumbens region (AL) of MPTP-treated monkeys. (M-N) In-vivo ^{18}F -FECNT SUR values in PET images and postmortem densitometry measurements of striatal TH-ir and DAT-ir parkinsonian monkeys were tightly correlated. The percentage changes of SUR in parkinsonian monkeys were calculated from their base line PET scans. TH and DAT immunostaining from control monkeys was used to calculate percent changes in densitometry measurements in parkinsonian monkeys. ROI values of each region (AL, PA, PM, CA) used in these correlations were collected from 5-7 coronal sections. Scale bars: A: 10 mm (valid for D,G and J); B: 3mm (valid for C, E,F,H,I,K and L).

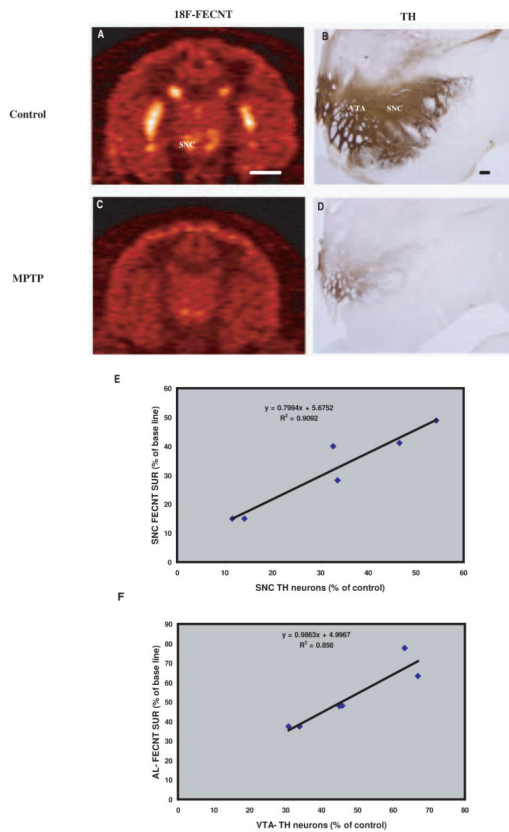


Fig. 6. Comparisons of in-vivo ^{18}F -FECNT PET images (A and C) with postmortem tyrosine hydroxylase immunoreactivity (B and D) in control (A and B) and MPTP-treated parkinsonian monkeys (C and D). (E) Correlation between in-vivo ^{18}F -FECNT SUR of substantia nigra (SN) and postmortem stereological SN cell count in parkinsonian monkeys. The parkinsonian monkeys SUR percentages were calculated from their base line PET scans in each hemisphere of three animals. Control monkeys stereological SN cell counts were used to calculate the percentage of dopaminergic cell loss in parkinsonian monkeys. Tight correlation was found between in-vivo ^{18}F -FECNT SN SUR and ex-vivo stereological SN cell count. (F) A significant correlation was found between in-vivo ^{18}F -FECNT SUR of Accumbens limbic (AL) and postmortem stereological VTA cell count in parkinsonian monkeys. Scale bars: A: 10 mm (valid for C); B: 2.5 mm (valid for D).

Table 1

Abbreviations

PET	Positron emission tomography
¹⁸ F-FECNT	2 β -carbomethoxy-3 β -(4-chlorophenyl)-8-(2-[¹⁸ F]-fluoroethyl)-nortropane
DAT	Dopamine transporter
TH	Tyrosine hydroxylase
PD	Parkinson's disease
DA	Dopamine
SERT	Serotonin transporter
NET	Norepinephrine transporter
MPTP	1-methyl-4-phenyl-1,2,3,6-tetrahydropyridine
ROI	Regions of interest
CE	Cerebellum
PA	Putamen associative
PM	Putamen motor
PL	Putamen limbic
CA	Caudate nucleus associative
AL	Nucleus accumbens limbic
SNC	Substantia nigra compacta
SUR	Specific uptake ratio
CB	Calbindin
ROD	Relative optical density
SNC-v	Substantia nigra pars compacta ventral
SNC-d	Substantia nigra pars compacta dorsal
VTA	Ventral tegmental area
TAC	Time activity curve
AADC	Aromatic acid decarboxylase
SPECT	Single photon emission computed tomography